

AGENT-BASED SIMULATION OF MOLECULAR PROCESSES

An Application to Actin-polymerisation

Stefan Pauleweit

Institute of Computer Science, Dept. of Systems Biology & Bioinformatics, University of Rostock, 18051 Rostock, Germany

J. Barbara Nebe

Center for Biomedical Research, Dept. of Cell Biology, University of Rostock, 18057 Rostock, Germany

Olaf Wolkenhauer

Institute of Computer Science, Dept. of Systems Biology & Bioinformatics, University of Rostock, 18051 Rostock, Germany

Keywords: Agent-based model, Actin polymerisation, Arp2/3, Systems biology.

Abstract: Agent-based modelling is widely used in ecology, economics and the social sciences. For the life science it is an increasingly used technology. Here we use agent-based modelling to simulate the formation of actin filaments, which is a major part in the cytoskeleton of the cell and plays a role in a number of cell functions. We present in this paper three models with different levels of detail and show the potential of agent-based models in systems biology by comparing the simulations to already published results.

1 INTRODUCTION

Agent-based simulations are a promising application emerging in life sciences (Merelli et al., 2007). Applications of agent-based technologies in systems biology include studies in which each cell is modelled as an agent (Thorne et al., 2007). Examples include bacterial chemotaxis (Emonet et al., 2005), the phenomenon where cells direct their movements in response to external signals, models of epidermal tissue (Grabe and Neuber, 2005), the formation of a 3D skin epithelium (Sun et al., 2009) or a hybrid model, and combination of agent-based simulations and differential equations to analyse the cell response to epidermal growth factors (Walker et al., 2006). Moreover, agent-based models for intracellular interactions representing the carbohydrate oxidation cell metabolism (Corradini et al., 2005), the cell cycle (Sütterlin et al., 2009), the NF- κ B signalling pathway (Pogson et al., 2008) and molecular self-organisation, with the focus on packing rigid molecules (Troisi et al., 2005), have been proposed.

Actin polymerisation is a molecular process that generates long filaments with a barbed and a pointed end from single actin molecules that become part of

the cytoskeleton. The cytoskeleton provides the physical structure and shape of cells, as well as plays an important role in a number of cell functions, including cell motility (Cooper, 1991; Pantaloni et al., 2001), endocytosis (Galletta et al., 2010), or cell division (Pelham and Chang, 2002). Understanding of actin organisation has important implications for practical medical applications, including the development of new topographies for implant surfaces (Matschegewski et al., 2010; Nebe et al., 2007).

Here we focus on the spatial and time dependent simulation of actin polymerisation. The literature describes a number of models analysing the cell motility driven by actin filaments, using partial differential equations (Mogilner and Edelstein-Keshet, 2002). Another study used Brownian dynamics to analyse the self-assembly process of actin and the dynamics of long filaments (Guo et al., 2009). The distribution of the length of actin filaments inside a cell was analysed with a discrete and continuous model (Edelstein-Keshet and Ermentrout, 1998). Different models using stochastic Π -calculus as a representative of process algebra, have also been published (Cardelli et al., 2009).

In this paper we describe simulations using

an agent-based approach with communicating X-machines (Gheorghe et al., 2005), implemented in a software called Flexible Large-scale Agent-based Modelling Environment (FLAME) (Kiran et al., 2008). This allows us to analyse the spatial and time dependent behaviour during the composition of the filament structure by free actin with a high degree of physical realism. The outline of the paper is as follows. Section 2 explains the three models in detail. Section 3 discusses the output of the models and Section 4 sums up the conclusions and gives a brief outlook for further studies.

2 AGENT-BASED SIMULATION

An agent is formally defined as a finite-state machine. Because the finite-state machine model is too restrictive for general system specification, an extension with a memory, the so called X-machine promise a better implementation (Holcombe, 1988). If a system contains more than one agent, the particular X-machines must be able to communicate together and this leads to a communication X-machine system (Gheorghe et al., 2005). This concept is implemented in the software named Flexible Large-scale Agent-based Modelling Environment (FLAME) (Kiran et al., 2008).

Using the actin model generated by X-ray analysis (Oda et al., 2009) we fix the size of one molecule to $50\text{\AA} \times 50\text{\AA}$. The dimension of the molecule is shown in Figure 1. Each agent contains an identification

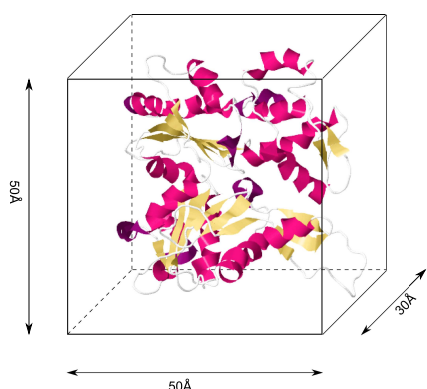


Figure 1: The physical size of the actin molecule determines the size of an agent in the simulation. For the two dimensional simulation the width and height of an actin agent is set to $50\text{\AA} \times 50\text{\AA}$ (Oda et al., 2009).

number and two binding sides to connect to another agent, namely bottom-bound (BB) and top-bound (TB) and can switch between three different states

(free, bottom-bound, fully bound). A free binding side is denoted with the constant -1 . As long as both binding sides are marked with -1 (free), the agent is randomly rotating and moving around in a distance of $1-200\text{\AA}$, which is an approximation for the computationally expensive calculation of Brownian dynamics. If a molecule binds to another, then the identification number of the counterpart is stored in the BB (respectively TB) variable; the agent becomes immobilised and its rotation will be adapted. The precondition for binding is, that one of the agents is already bound (bottom-bound). This leads to the condition that at least one agent has to be stuck in the beginning of the simulation. This is done by initialising one agent with $BB = 0$. If a free agent binds to an already bound one, the second becomes then fully bound ($BB \neq -1$, $TB \neq -1$). The whole schema of the actin-actin interactions is also shown in Figure 2. The polymerisa-

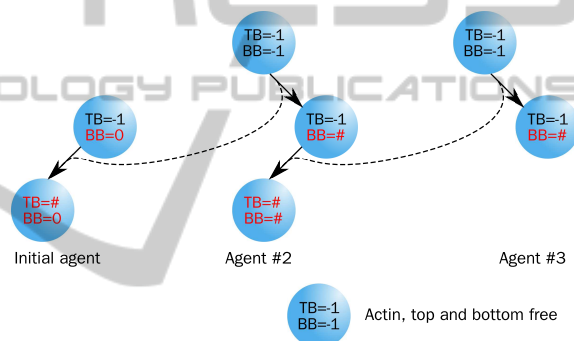


Figure 2: An actin-agent can be in three different states. A free molecule can bind to an already bound initial agent ($BB = 0$). The already bound actin-agent then become fully bound. Then the third actin-agent can bind to the second actin-agent which become fully bound and so on.

tion of actin filaments is characterised by a 70° angle branching on several positions mediated by the Arp2/3 protein (Stossel et al., 2006). To simulate this branching process, a new agent with a third binding side was implemented. The orientation of the branching side to the left or right was set randomly. This agent is restricted to bind only to actin-agents, so that a Arp2/3-Arp2/3 combination is prohibited. In Figure 3 the scheme for the interactions and state changes is illustrated. Similar to the actin-agent, the size of this agent was determined from published measurements (Robinson et al., 2001). Figure 4 shows the approximated dimensions of Arp2/3. An agent-based model has to include the reaction kinetic in a reasonable way. Due to the nature of spatial simulations with individual molecules, this may be done by an interaction volume, which defines a reaction zone around a particular agent (see Figure 5). Andrews and Bray (2004)

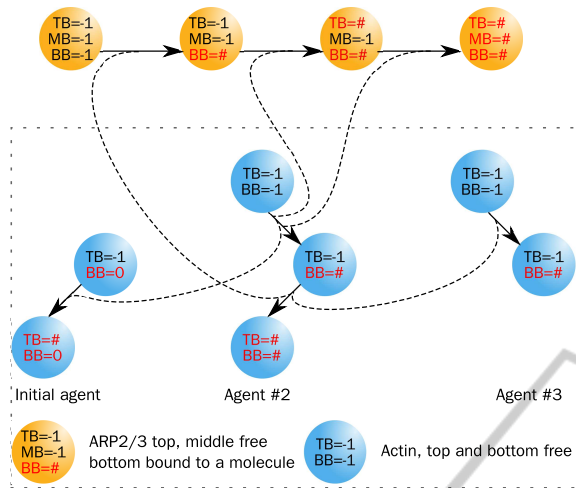


Figure 3: In addition to the actin-agent (Figure 2), the simulation was extended with a second type of agent for Arp2/3. This agent can bind to an bottom-bound actin-agent. Then another actin-agent can bind to the top-binding side of the Arp2/3-agent, the next actin-agent to the middle binding side and the Arp2/3-agent becomes fully bound.

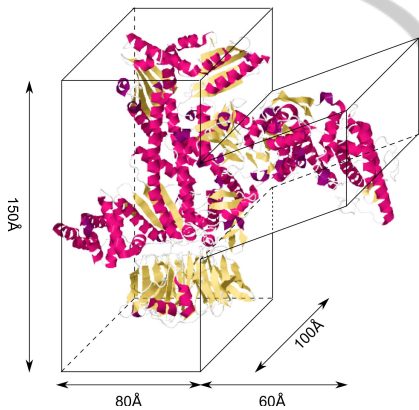


Figure 4: The physical size of Arp2/3 determines the size of the agents in the simulation (Robinson et al., 2001).

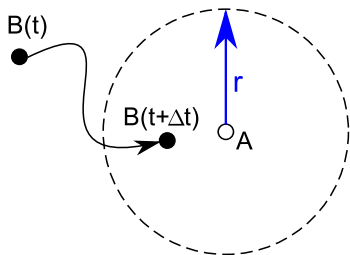


Figure 5: The interaction boundary (dashed circle) defines the reaction volume around an agent. If a second agent enters this area, the reaction takes place.

developed an algorithm to determine this volume, but considered more detailed interactions. Another way

is described by Pogson et al. (2006) where the interaction radius r is calculated by:

$$r = \sqrt[3]{\frac{3k\Delta t}{4\pi N_A 10^3}}$$

where k is the kinetic rate constant, Δt the discrete time interval and N_A is Avogadro's constant (6.022×10^{23}). The rate constant for actin-actin assembly was determined with $11.6 \mu M^{-1} s^{-1}$ (Fujiwara et al., 2007) and leads to a radius of 0.166 \AA for $\Delta t = 1 s$. If two or more agents enter the interaction volume at the same time step, the closest molecule to the reaction molecule assembles to it, if two or more have the same distance, one will be chosen by chance.

To compare our results with the simulation of Cardelli et al. (2009), we used the same number of 1200 free actin agents and 30 Arp2/3 agents. Cardelli uses this number of agents to simulate a concentration of $1200 \mu M$. For concentration values in a spatial simulations, it is necessary to calculate the volume of the environment:

$$n_{\text{Actin}} = N_A \times V \times c \quad [1/\text{mol} \times l \times \text{mol}/l]$$

$$V = 1200 / (N_A \cdot 1200 \times 10^{-6})$$

$$V = 1.66 \times 10^{-18} l = 1.66 \times 10^{-21} m^3$$

where n_{Actin} is the number of molecules, N_A is again Avogadro's constant, c is the concentration of molecules and V is the volume. Assuming the environment as a cube, the length of a side is approximately 1184.0 \AA .

For a simulation including the dissolving of actin from a filament, we used the rate constant of $5.4 s^{-1}$ for ADP-actin at the barbed end from the literature (Fujiwara et al., 2007). Only agents with a free top-bound (in case of Arp2/3 also middle bound) can be released from the filament. To avoid an instant re-coupling, the molecule will be moved to outside the interaction boundary.

Our present agent-based simulation takes place in a 2D environment, so that we have to introduce a factoring constant of 100 for the radius, the dissolving rate constant and the size of the environment, following the paper of Cardelli et al. (2009).

3 RESULTS

3.1 Actin-Actin Interactions

Figure 6 shows the time plot of the growth of one filament. The curve shows in the beginning a linear increase (see inset of Figure 6), but later becomes logarithmic. After 390 seconds 50 agents were integrated

in the filament, which corresponds to a filament of length $0.25\mu\text{m}$. A length of $1\mu\text{m}$ is reached after 1882 seconds and at the end of one hour, 240 agents form a filament with a length of $1.2\mu\text{m}$. In agreement with

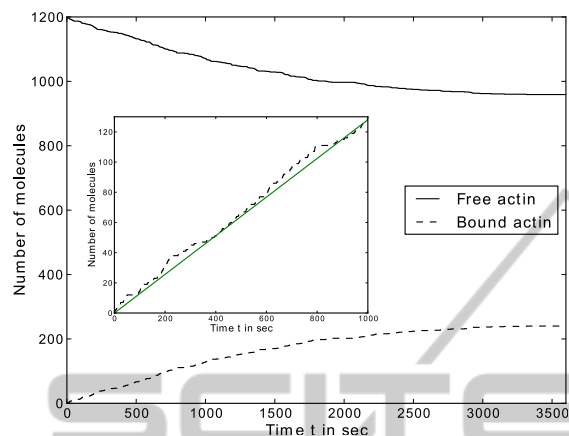


Figure 6: The time plot shows the result of the simulation for a simple actin polymerisation with 1200 agents and a time step $\Delta t = 1s$. Inset: Linear slope of the binding process in the beginning.

published measurements (Fujiwara et al., 2007), the increase in length of actin is linear in the beginning of the simulation. The logarithmic curve on can be explained by the decreased number of free molecules and the spatial phenomena, by which the simulated filament is growing close to the boundary of the environment. The number of reachable free molecules close to this boundary is then much lower. The difference in the speed of elongation is related to two reasons:

1. Actin filaments can growth on both side, whereas the simulation allows only the growth at the barbed end.
2. Actin can build small motile fragments, which then elongate the filament (Stossel et al., 2006). This increases the speed of polymerisation significantly.

3.2 Branching Process

Adding a new agent for the Arp2/3 protein, we simulated the actin polymerisation with the branching process. To visualise this, Figure 7 shows a snapshot of the spatial distribution at the end of one hour. In this simulation an overall filament length of $1\mu\text{m}$ was reached after 578 seconds. At the end of one hour, nearly all agents were involved in the filament structure, 1121 actin agents were fully bound. Additionally 28 Arp2/3 agents are fully bound, two of them

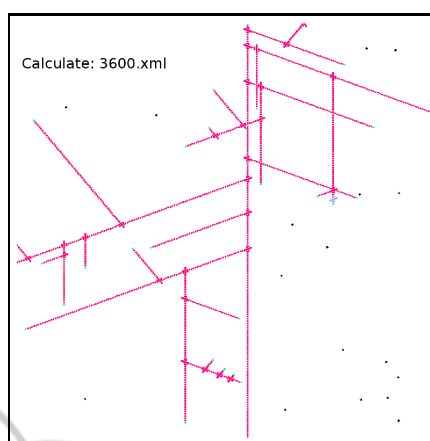


Figure 7: The figure (cropped for better illustration) shows the end result of the simulation for one hour with 1200 actin-agents and 30 Arp2/3-agents. The black points mimic the free actin, the blue the agents bind to the filamental structure.

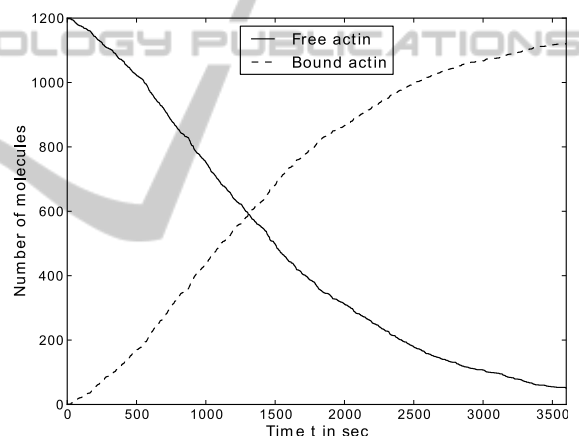


Figure 8: The time plot shows the result of the branching simulation for actin of 1200 actin-agents, 30 Arp2/3-agents and a time step $\Delta t = 1s$.

had an open binding side. Figures 8 and 9 show the time plots for the actin and arp agents respectively. Both time curves are sigmoidal with an inflection point around 1300 seconds.

In contrast to the filament formation, solely with actin, the branching process accelerate the elongation significantly. The snapshot in Figure 7 shows the spatial consideration and is in good agreement with previously published simulations (Cardelli et al., 2009, Figure 17).

3.3 Disassembly Process

To model the disassembly of actin and Arp2/3 molecules from the filamental structure, we added a

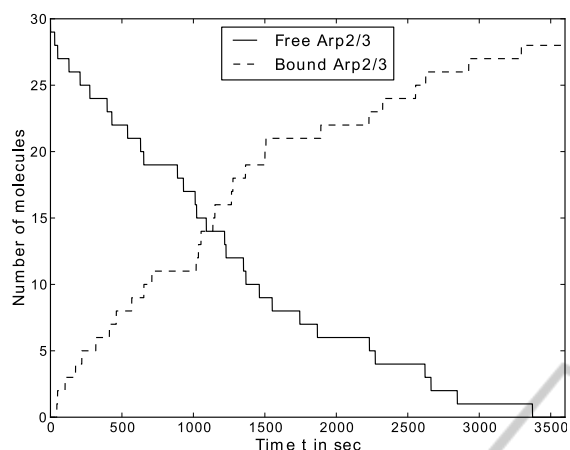


Figure 9: The time plot shows the result of the branching simulation for Arp2/3 with 1200 actin agents, 30 Arp2/3 agents and a time step $\Delta t = 1s$.

new probability for each agent.

After introducing this new variable, the assembly of

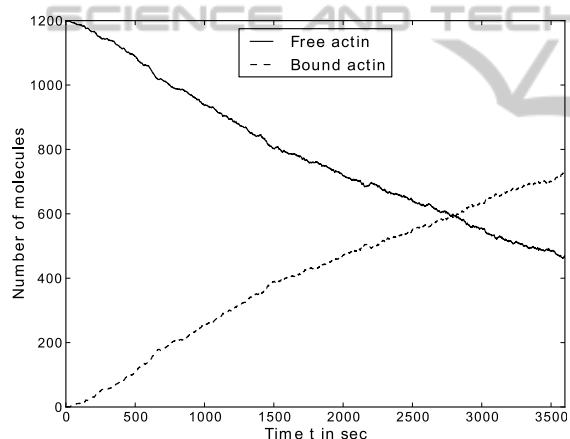


Figure 10: The time plot shows the result of the branching simulation, including the disassembly process, for actin of 1200 actin-agents, 30 Arp2/3-agents and a time step $\Delta t = 1s$.

the actin filament slowed down. As shown in Figure 10, the assembly of 200 molecules and therefore an overall length of $1\mu m$ is reached after 760 seconds. After one hour, the filament contained 717 fully bounded actin-agents and is branched out at 14 different positions (see also Figure 11). This model shows therefore a comparable time progression to the simulation of Cardelli et al. (2009), especially for Arp2/3, although our filamental growth is somewhat slower.

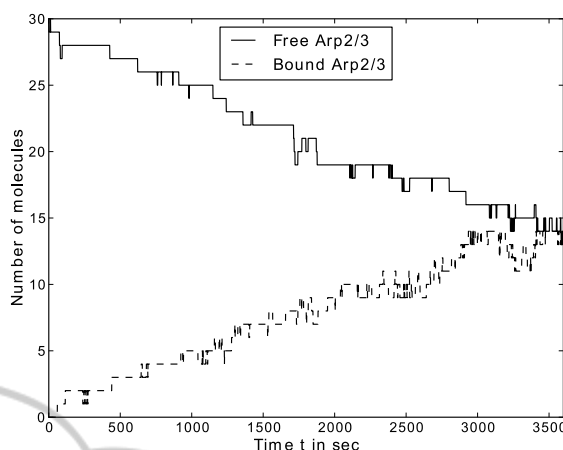


Figure 11: The time plot shows the result of the branching simulation, including the disassembly process, for actin of 1200 actin-agents, 30 Arp2/3-agents and a time step $\Delta t = 1s$.

4 CONCLUSIONS AND OUTLOOK

Instead of the commonly used rate equations to simulate intracellular molecular processes, we introduced an agent-based approach. This allowed us to overcome some restrictions imposed by differential equation models, more precisely any number and any distribution, as well as spatial behaviour of molecules can be easily modelled. Our model simulates actin polymerisation, an important key player for different cell functions.

The spatial outcome of our model is comparable to alternative models of Cardelli et al. (2009), using the stochastic Π -calculus. Because the FLAME-framework produces XML-files for each time step, we are also able to create an animated version for tracking the filament formation (not shown here). Additionally a time dependent analysis of the behaviour of the single molecules and the filaments can be done. The limit in using the agent-based approach is only given by computational purposes.

Our overall aim is the development of a biophysical realistic model for actin polymerisation in human cells. The advantage of our approach is the possibility to extend the simulation to a massive number of molecules with the aid of the parallelised FLAME software version and, more important, the easy implementation of external influences. This should enable us to analyse observed phenomena of actin clustering on titan pillar surface structures (Matschegewski et al., 2010) with applications to implant technologies. This interesting issue makes it necessary to in-

clude more proteins like capping proteins which stop the elongation of the filament (Pollard and Cooper, 1986).

ACKNOWLEDGEMENTS

We are grateful for financial support of the research training school “Welisa”, which is founded by the German Research Foundation (DFG 1505/1). Furthermore the authors are thankful for the helpful advice of Prof. Mike Holcombe and Mark Burkitt from the University of Sheffield.

REFERENCES

- Andrews, S. S. and Bray, D. (2004). Stochastic simulation of chemical reactions with spatial resolution and single molecule detail. *Phys. Biol.*, 1(3-4):137–151.
- Cardelli, L., Caron, E., Gardner, P., Kahramanoğlu, O., and Phillips, A. (2009). A process model of actin polymerisation. *Electronic Notes in Theoretical Computer Science*, 229(1):127–144. Proceedings of the Second Workshop From Biology to Concurrency and Back (FBTC 2008).
- Cooper, J. A. (1991). The role of actin polymerization in cell motility. *Annu. Rev. Physiol.*, 53:585–605.
- Corradini, F., Merelli, E., and Vita, M. (2005). A multi-agent system for modelling carbohydrate oxidation in cell. In Gervasi, O., Gavrilova, M., Kumar, V., Laganà, A., Lee, H., Mun, Y., Taniar, D., and Tan, C., editors, *Computational Science and Its Applications – ICCSA 2005*, volume 3481 of *Lecture Notes in Computer Science*, pages 227–247. Springer Berlin / Heidelberg.
- Edelstein-Keshet, L. and Ermentrout, G. B. (1998). Models for the length distributions of actin filaments: I. simple polymerization and fragmentation. *Bull. Math. Biol.*, 60(3):449–475.
- Emonet, T., Macal, C. M., North, M. J., Wickersham, C. E., and Cluzel, P. (2005). Agentcell: a digital single-cell assay for bacterial chemotaxis. *Bioinformatics*, 21(11):2714–2721.
- Fujiwara, I., Vavylonis, D., and Pollard, T. D. (2007). Polymerization kinetics of adp- and adp-pi-actin determined by fluorescence microscopy. *Proc. Natl. Acad. Sci. U. S. A.*, 104(21):8827–8832.
- Galletta, B. J., Mooren, O. L., and Cooper, J. A. (2010). Actin dynamics and endocytosis in yeast and mammals. *Curr. Opin. Biotechnol.*, in Press.
- Gheorghe, M., Stamatopoulou, I., Holcombe, M., and Kefalas, P. (2005). Modelling dynamically organised colonies of bio-entities. In Banâtre, J.-P., Fradet, P., Giavitto, J.-L., and Michel, O., editors, *Unconventional Programming Paradigms*, volume 3566 of *Lecture Notes in Computer Science*, pages 207–224. Springer Berlin / Heidelberg.
- Grabe, N. and Neuber, K. (2005). A multicellular systems biology model predicts epidermal morphology, kinetics and ca²⁺ flow. *Bioinformatics*, 21(17):3541–3547.
- Guo, K., Shillcock, J., and Lipowsky, R. (2009). Self-assembly of actin monomers into long filaments: Brownian dynamics simulations. *J. Chem. Phys.*, 131(1):015102.
- Holcombe, M. (1988). X-machines as a basis for dynamic system specification. *Softw. Eng. J.*, 3(2):69–76.
- Kiran, M., Coakley, S., Walkinshaw, N., McMin, P., and Holcombe, M. (2008). Validation and discovery from computational biology models. *Biosystems*, 93(1-2):141–150.
- Matschegewski, C., Staehlke, S., Loeffler, R., Lange, R., Chai, F., Kern, D. P., Beck, U., and Nebe, B. J. (2010). Cell architecture-cell function dependencies on titanium arrays with regular geometry. *Biomaterials*, 31(22):5729–5740.
- Merelli, E., Armano, G., Cannata, N., Corradini, F., d’Inverno, M., Doms, A., Lord, P., Martin, A., Milanesi, L., Möller, S., Schroeder, M., and Luck, M. (2007). Agents in bioinformatics, computational and systems biology. *Brief. Bioinform.*, 8(1):45–59.
- Mogilner, A. and Edelstein-Keshet, L. (2002). Regulation of actin dynamics in rapidly moving cells: a quantitative analysis. *Biophys. J.*, 83(3):1237–1258.
- Nebe, J. G. B., Luethen, F., Lange, R., and Beck, U. (2007). Interface interactions of osteoblasts with structured titanium and the correlation between physicochemical characteristics and cell biological parameters. *Macromol. Biosci.*, 7(5):567–578.
- Oda, T., Iwasa, M., Aihara, T., Maéda, Y., and Narita, A. (2009). The nature of the globular- to fibrous-actin transition. *Nature*, 457(7228):441–445.
- Pantaloni, D., Clainche, C. L., and Carlier, M. F. (2001). Mechanism of actin-based motility. *Science*, 292(5521):1502–1506.
- Pelham, R. J. and Chang, F. (2002). Actin dynamics in the contractile ring during cytokinesis in fission yeast. *Nature*, 419(6902):82–86.
- Pogson, M., Holcombe, M., Smallwood, R., and Qwarnstrom, E. (2008). Introducing spatial information into predictive nf-kappab modelling—an agent-based approach. *PLoS One*, 3(6):e2367.
- Pogson, M., Smallwood, R., Qwarnstrom, E., and Holcombe, M. (2006). Formal agent-based modelling of intracellular chemical interactions. *Biosystems*, 85(1):37–45.
- Pollard, T. D. and Cooper, J. A. (1986). Actin and actin-binding proteins. a critical evaluation of mechanisms and functions. *Annu. Rev. Biochem.*, 55:987–1035.
- Robinson, R. C., Turbedsky, K., Kaiser, D. A., Marchand, J. B., Higgs, H. N., Choe, S., and Pollard, T. D. (2001). Crystal structure of arp2/3 complex. *Science*, 294(5547):1679–1684.
- Stossel, T. P., Fenteany, G., and Hartwig, J. H. (2006). Cell surface actin remodeling. *J. Cell Sci.*, 119(Pt 16):3261–3264.

- Sütterlin, T., Huber, S., Dickhaus, H., and Grabe, N. (2009). Modeling multi-cellular behavior in epidermal tissue homeostasis via finite state machines in multi-agent systems. *Bioinformatics*, 25(16):2057–2063.
- Sun, T., Adra, S., Smallwood, R., Holcombe, M., and MacNeil, S. (2009). Exploring hypotheses of the actions of *tgf-beta1* in epidermal wound healing using a 3d computational multiscale model of the human epidermis. *PLoS One*, 4(12):e8515.
- Thorne, B. C., Bailey, A. M., and Peirce, S. M. (2007). Combining experiments with multi-cell agent-based modeling to study biological tissue patterning. *Brief. Bioinform.*, 8(4):245–257.
- Troisi, A., Wong, V., and Ratner, M. A. (2005). An agent-based approach for modeling molecular self-organization. *Proc. Natl. Acad. Sci. USA*, 102(2):255–260.
- Walker, D., Wood, S., Southgate, J., Holcombe, M., and Smallwood, R. (2006). An integrated agent-mathematical model of the effect of intercellular signalling via the epidermal growth factor receptor on cell proliferation. *J. Theor. Biol.*, 242(3):774–789.

